Journal of the American Association for Laboratory Animal Science
Copyright 2011
by the American Association for Laboratory Animal Science

Vol 50, No 3
May 2011
Pages 326–336

Eliminating Animal Facility Light-at-Night Contamination and Its Effect on Circadian Regulation of Rodent Physiology, Tumor Growth, and Metabolism: A Challenge in the Relocation of a Cancer Research Laboratory

Robert T Dauchy,[1,3,*] Lynell M Dupepe,[2] Tara G Ooms,[2] Erin M Dauchy,[1] Cody R Hill,[1] Lulu Mao,[1] Victoria P Belancio,[1] Lauren M Slakey,[1] Steven M Hill,[1] and David E Blask[1]

Appropriate laboratory animal facility lighting and lighting protocols are essential for maintaining the health and wellbeing of laboratory animals and ensuring the credible outcome of scientific investigations. Our recent experience in relocating to a new laboratory facility illustrates the importance of these considerations. Previous studies in our laboratory demonstrated that animal room contamination with light-at-night (LAN) of as little as 0.2 lx at rodent eye level during an otherwise normal dark-phase disrupted host circadian rhythms and stimulated the metabolism and proliferation of human cancer xenografts in rats. Here we examined how simple improvements in facility design at our new location completely eliminated dark-phase LAN contamination and restored normal circadian rhythms in nontumor-bearing rats and normal tumor metabolism and growth in host rats bearing tissue-isolated MCF7(SR$^-$) human breast tumor xenografts or 7288CTC rodent hepatomas. Reducing LAN contamination in the animal quarters from 24.5 ± 2.5 lx to nondetectable levels (complete darkness) restored normal circadian regulation of rodent arterial blood melatonin, glucose, total fatty and linoleic acid concentrations, tumor uptake of O_2, glucose, total fatty acid and CO_2 production and tumor levels of cAMP, triglycerides, free fatty acids, phospholipids, and cholesterol esters, as well as extracellular-signal-regulated kinase, mitogen-activated protein kinase, serine–threonine protein kinase, glycogen synthase kinase 3β, γ-histone 2AX, and proliferating cell nuclear antigen.

Abbreviations: 13-HODE, 13-hydroxyoctadecadienoic acid; γH2AX, histone 2AX; AKT, serine–threonine protein kinase; ERK1/2, extracellular signal-regulated kinase p44/46; GSK3β, glycogen synthase kinase 3β: LAN, light at night; MEK, mitogen-activated protein kinase kinase, PCNA, proliferating cell nuclear antigen; SR$^-$, steroid-receptor–negative.

Relocating laboratory animal research from one institution to another can be a daunting task for both scientists and animal care personnel with regard to control of lighting and elimination of light-at-night (LAN) contamination. Appropriate facility lighting and lighting protocols, as outlined in the *Guide for the Care and Use of Laboratory Animals*,[30] are essential for maintaining the health and wellbeing of laboratory animals and ensuring the credible outcome of scientific investigations.[16-18,22] The profound effect of light on circadian behavior and physiology is well established.[2,3,5,9,11,12,16-18,22,29,32,44,46,49,52,55-58,64]

Minor alterations in light intensity,[11] spectral quality,[12] and duration[9] at any given time of day can alter or disrupt chronobiologic rhythms markedly in all mammals.[6,17,26,44,55-59] Light information, which initially is detected by a small group of intrinsically photosensitive retinal ganglion cells containing the blue light-sensitive photopigment melanopsin,[6,26] is transmitted through the retinohypothalamic tract[59] to a central molecular clock located in the suprachiasmatic nucleus of the hypothalamus.[32,57] The suprachiasmatic nucleus, the activity of which is entrained by the light:dark cycle,[32,57] sends projections over a polysynaptic pathway to the pineal gland driving a series of molecular events leading to the production of the pineal neurohormone melatonin (N-acetyl-5 methoxytryptamine), primarily during the night.[29,46] The daily rhythmic melatonin signal contributes to the temporal coordination of normal behavioral and physiologic functions including the sleep–wake[23,46,66] and reproductive cycles,[51,55] immune function,[38,41,56] hormone levels,[19,31,45,47,68] temperature regulation,[23] electrolyte balance,[69] neural protein synthesis,[65] and redox states.[24,53]

Dark-phase LAN exposure suppresses endogenous melatonin concentrations and may lead to various disease states,[42,58] including carcinogenesis,[7,8,16,18,33] and metabolic syndrome.[17,34-37,39,70] Previous in vivo studies in our former laboratory (at the Bassett Research Institute, Cooperstown, NY) demonstrated that animal room LAN of as little as 0.2 lx (0.08 μW/cm^2; rodent eye level) during an otherwise normal dark-phase suppressed normal physiologic nighttime melatonin levels, leading to markedly disrupted circadian regulation of physiology and metabolism in nontumor-bearing host animals[16,18] and a stimulation in metabolism and proliferation of both tissue-isolated MCF7 steroid-receptor–negative (SR$^-$) human breast cancer xenografts and syngeneic grafts of rodent hepatoma 7288CTC in rats.[7,17] This effect was mediated by melatonin receptor-mediated sup-

Received: 08 Oct 2010. Revision requested: 13 Dec 2010. Accepted: 15 Dec 2010.
Departments of [1]Structural and Cellular Biology and [2]Comparative Medicine, Tulane University School of Medicine, Tulane, Louisiana.
[*]Corresponding author. Email: rdauchy@tulane.edu.

pression of cAMP, leading to inhibition of tumor linoleic acid uptake and its metabolism to the mitogenic signaling molecule 13-hydroxyoctadecadienoic acid (13-HODE). These events culminated in downregulation of epidermal growth factor and insulin-like growth factor 1 pathways.[7,8,16-19,62]

Exposure to LAN is likely to exert pervasive and problematic effects on mammalian behavior and physiology in laboratory animal facilities around the world. During the past decade, improved facility design and better adherence to animal room lighting protocols certainly has helped to reduce the problem. In moving to our laboratory animal facility at Tulane University School of Medicine (New Orleans, LA), we discovered considerable preexisting LAN contamination that had to be eliminated before we could resume our human cancer research.

The current study was performed to monitor the effects of the elimination of animal room LAN contamination over time on animal health and wellbeing, tumor growth, and metabolic profiles by assessing well-established circadian parameters in physiology and metabolism.[7,8,16-18] We measured light-induced suppression of melatonin, an accepted and sensitive marker of the effects of light on the circadian system in all mammals,[2,3,5,9,11,12,15,16,18,20,21,29,44,46,49,52,55-58,64] before and after tumor implantation and growth. Tissue-isolated MCF7(SR^-) human breast cancer xenografts and 7288CTC rat hepatomas have been well-characterized over the years in our former light-tight facilities[7,8,16-18] and provided us with unique markers and measures of the extent to which LAN contaminated our new animal quarters. In tumor-bearing animals exposed to even minimal LAN, the latency-to-onset of tumor growth and proliferation rates of these tumors increase markedly in direct proportion to LAN intensity. As improvements were made to eliminate LAN contamination in the new location over the course of more than 20 generations of tumor passages, we measured the changes and reestablishment of normal rat and host–tumor circadian regulation. The information from this study may assist investigators and animal care personnel in addressing this important influence on the health and wellbeing of laboratory animals and consequent effects on the outcome of scientific investigations.

Materials and Methods

Reagents. HPLC-grade chloroform, ethyl ether, methanol, glacial acetic acid, heptane, hexane, and Sep-Pak C18 cartridges for HPLC extraction of samples were purchased from Fisher Chemical (Pittsburgh, PA). Free fatty acid, cholesterol ester, triglyceride, phospholipid, rapeseed oil, and methyl ester standards; boron trifluoride–methanol; and perchloric and trichloroacetic acids were purchased from Sigma Scientific (St Louis, MO). The HPLC standards, (±)5-hydroxyeicosatetraenoic acid (catalog no. 34210) and 13(S)-HODE (catalog no. 38610), and ultrapure water (catalog no. 400000) were purchased from Cayman Chemical (Ann Arbor, MI).

Animals, housing conditions, facility modifications and improvements, and diet. Over the course of the 18 mo of this study, 46 adult female, homozygous, athymic, inbred nude rats (Hsd:RH-*Foxn1*^{rnu}; Harlan, Indianapolis, IN) and 52 adult male Buffalo rats (BUF/CrCrl; Charles River, Wilmington, MA) were evaluated. Both strains were SPF for Sendai virus, pneumonia virus of mice, sialodacryoadenitis virus, Kilham rat virus, Toolan H1 virus, Theiler murine encephalomyelitis virus, reovirus, *Mycoplasma pulmoni,* lymphocytic choriomeningitis virus, mouse adenovirus 1 and 2, Hantaan virus, *Encephalitozoon cuniculi,* cilia-associated respiratory bacillus, parvovirus NS1, rat parvoviruses, and rat murine virus. Rats were maintained in environmentally controlled rooms (25 °C; 50% to 55% humidity) with diurnal lighting [12:12 (light:dark); lights on 0600; 125 lx; 304 μW/cm^2].

Animal rooms were lighted with a series of 3 overhead ballast–lamp systems each containing 4 cool-white fluorescent lamps (Philips F32T8TL741, Alto Collection 32W, Somerset, NJ); the same fluorescent lamps were used in the constantly lighted corridors. During the transition period, modifications and improvements were made, which included removal of lighted equipment; installation of doorframe shoes, seals, and sweeps with vinyl gaskets and anodized aluminum encasements (National Guard Products, Memphis, TN); improved lighting protocols; and implementation of laboratory animal technician education and training sessions (occurred during tumor passages F1 to F9). During the final stage of dark-phase light decontamination (during the F9 tumor passage), exterior lightproof 'dark' curtains (Davis Contract Draperies, Harahan, LA) were installed. These curtains provided an occlusive seal around the entire door and doorframe that linked a constantly lighted work corridor to the animal rooms themselves. Weekly and during all modifications and improvements to the animal facilities, rooms were monitored for normal light-phase lighting intensities and LAN contamination at 1 m above the floor in the center of each room (rodent eye level) from within and at the front of the animal cages by using a radiometer–photometer (model no. IL1400A) and detector (model no. SEL033; both from International Light Technologies, Peabody, MA); these instruments were calibrated regularly throughout the course of this study.

In a separate experiment and for comparison, dark-phase LAN contamination was measured in animal facilities that were traditional in design and had an entry door with a standard 10 in. × 12 in. translucent window that looked onto a constantly lighted corridor. Dark-phase light entry was measured at 1 m above the floor and inside a rodent cage positioned at eye level on a cage rack at 9 ft from the door, as well as in the outside lighted corridor. In addition, photoperiods and lighting levels were monitored daily by using in-room lighting sensors for each light level in conjunction with photocell sensors to monitor extraneous room dark-phase lighting due to inappropriate entry or lighting malfunctions due to mechanical failure.

To ensure that all animals remained infection-free from both bacterial and viral agents, serum samples from sentinel rats were tested quarterly for excluded agents (listed earlier) throughout the course of this study by ELISA (Research Animal Diagnostic Laboratory, Columbia, MO) throughout the course of this investigation. Animals were given free access to food (Purina 5053 Irradiated Laboratory Rodent Diet, PMI, Richmond, IN) prepared in accordance with national standards,[48] and acidified water. Quadruplicate determinations of this diet contained 4.1 g total fatty acid per 100 g of diet, composed of 0.04% myristic (C14:0), 12.50% palmitic (C16:0), 0.24% palmitoleic (C16:1n7), 3.12% stearic (C18:0), 21.70% oleic (C18:1n9), 56.13% linoleic (C18:2n6), 5.80% γ-linolenic, and 0.23% arachidonic (C20:4n6) acids. Minor amounts of other fatty acids comprised 0.24%. Conjugated linoleic acids and trans fatty acids were not found. More than 90% of the total fatty acids was in the form of triglycerides; more than 5% was in the form of free fatty acids. Animals were maintained in an AAALAC-accredited facility in accordance with *The Guide for the Care and Use of Laboratory Animals*.[30] All procedures for animal use were approved by the IACUC.

Arterial blood collection. After at least a 2-wk exposure to the lighting regimens described earlier, nontumor-bearing rats to be used for each subsequent generation of tumor xenograft implants underwent 2 low-volume blood draws by cardiocen-

tesis to collect arterial blood, as described previously,[8,16-19] over 14 d prior to tumor implantation. Briefly, blood was collected at either 0400 (nighttime) or 1600 (daytime); each animal was tested only once every 4 to 5 d to eliminate potential effects on feeding, stress, and potential mortality. Animals were lightly anesthetized by CO_2 inhalation (70% CO_2, 30% air); 0.5-mL arterial blood samples (less than 5% total blood volume) were taken from the left ventricle by cardiocentesis with tuberculin syringes (25-gauge, 3/8 in.; Becton-Dickinson, Franklin Lakes, NJ) moistened with sodium heparin (1000 U/mL; APP Pharmaceuticals, Schaumburg, IL); 65 µL was taken for blood acid–gas analysis (iSTAT1 Analyzer, Abbott; CG8+ cartridges, Heska Corporation, Loveland, CO) on samples after acquisition of the analyzer (following facility modifications and elimination of LAN). Cardiocentesis blood samples acid–gas values were compared with those collected during the arterio(carotid artery)–venous tumor measurements to ensure the arterial nature of the blood collected. Blood sampling during the dark-phase (that is, at 0400) was completed under a safelight red lamp (1A, model B, catalog no. 152 1517; 120 V, 15 W; Kodak, Rochester, NY) to preserve the nocturnal melatonin surge.[7,9,14,15,40,71]

Melatonin analysis. Arterial plasma melatonin levels measured by using a sensitive rat ^{125}I melatonin radioimmunoassay kit (catalog no. BA 3500, Labor Diagnostika Nord, Nordham, Germany) and analyzed by using an automated gamma counter (Packard Cobra 5005, Hewlett-Packard, Palo Alto, CA), as previously described.[7] The minimal detection level for the assay was 1 to 2 pg/mL plasma.

Tumor xenograft implantation and growth measurements. MCF7(SR$^-$) human breast cancer xenografts were implanted into nude rats and Morris rat hepatoma 7288CTC syngeneic grafts were implanted into Buffalo rats and grew as previously described.[7,8,16-18,61,62] The human cancer xenografts and syngeneic grafts grew as tissue-isolated tumors with a single arterial and venous connection to the host. Latency-to-onset of tumor growth was noted, and estimated tumor weights were measured and recorded, as previously described.[16,17,61]

Tumor xenograft arteriovenous difference measurements. When tumors reached an estimated 5 to 7 g in weight, rats were prepared for arterial and venous blood measurements between 0600 and 0700. Rats were anesthetized with ketamine–xylazine solution (89.1 mg/kg and 9.9 mg/kg IP), and arterial and venous blood samples were collected from the tissue-isolated tumor xenografts, as previously described.[61] Samples of arterial and venous blood were taken for hematocrit determination and blood acid–gas and glucose analysis (iSTAT1 Analyzer, Abbott). At the end of collection, all rats were exsanguinated through the carotid catheter.

Fatty acid extraction and analysis, tumor 13-HODE production, and determination of tumor cAMP levels. Arterial plasma total fatty acids were extracted from 0.1-mL arterial and venous samples after the addition of heptadecanoic acid (C17:0), as described previously.[7,8,16,18,57,58] Tumor tissue total fatty and linoleic acid levels in control and treatment groups were extracted from 0.1 mL of 20% homogenates, as previously described.[7,8,16,18,57,58] Contents are reported here as micrograms per gram of tumor (wet weight). Tumor total fatty acids and fatty acid lipid fractions, that is, triglycerides, phospholipids, free fatty acids, and cholesterol esters were separated by using silica gel G plates (Uniplate no. 01011; Alltech, Newark, DE), as described previously.[7,8,16,18,57,58] Analyses were performed in duplicate. Methyl esters of the fatty acids were analyzed by using a gas chromatograph (model no. HP 5890A, Hewlett-Packard) equipped with a fused-silica capillary column (no. 2330; 30 m × 0.25 mm, 0.25-µm film thickness; Supelco, Bellefonte, PA), as described previously.[16,18,61] Values for total fatty acids represent the sum of the 7 major fatty acids (myristic, palmitic, palmitoleic, stearic, oleic, linoleic, and arachidonic acids) in the blood plasma as free fatty acids, cholesterol esters, triglycerides, phospholipids, and other plasma lipids and are expressed here as micrograms or milligrams per liter plasma. Physiologic levels of total fatty acids in different batches of donor arterial blood collected from fed rats differed by as much as 10%. Analyses showed this variation slightly altered the rates of total fatty acid and linoleic acid uptake in tumor somewhat but not the rate of uptake as a percentage of supply to the tumor, which remained consistent at about 17% to 20%. For statistical comparisons, rates of total fatty and linoleic acid uptakes are presented here both as absolute values [micrograms per minute per g tumor (wet weight)] and as percentage of supply (defined as total fatty or linoleic acid uptake / arterial supply × 100%). Tumor production of 13-HODE was measured as previously described, by using 0.2-mL arterial and venous plasma samples, and are reported here as nanograms per minute per gram wet weight.[16,18,62] Tumor levels of cAMP were determined by means of ELISA (GE Lifesciences, Piscataway, NJ) as described previously and are reported as nanomoles per gram wet weight.[7,8,62]

Western blot measurement of tumor phosphorylated kinases. The frozen tumor tissue was ground into fine powder; lysed in Tissue Extraction Reagent I (catalog no. FN0071; Invitrogen, Camarillo, CA) containing Tris (50 mM, pH 7.4), EDTA (20 mM), NP40 (0.5%), NaCl (150 mM), phenylmethylsulfonyl fluoride (0.3 mM), NaF (1 mM), $NaVO_4$ (1 mM), dithiothreitol (1mM) and protease and phosphatase inhibitor cocktails [protein: protease–phosphatase inhibitor, 100: 1 (v/v)]; and homogenized by hand (Potter–Elvehjem tissue grinding tube with homogenizer, Wheaton Science Products, Millville, NJ). The tissue lysates were centrifuged for 10 min at 10,000 × *g*, 4 °C. Protein concentrations of the supernatants were determined by using a protein assay kit (Bio-Rad, Hercules, CA). Total protein (90 µg per sample) was separated electrophoretically on a 12% SDS–polyacrylamide gel, and electroblotted onto a membrane (Hybond, GE Healthcare, Piscataway, NJ). After incubation with 5% nonfat milk in Tris-buffered saline containing 0.05% Tween, immunoblots were probed with antibodies to phosphorylated extracellular signal-regulated kinase p44/42 (ERK 1/2; Thr202/Tyr204), phosphorylated mitogen-activated protein kinase kinase (MEK1/2; Ser217/Ser221), phosphorylated serine–threonine protein kinase (AKT; Ser473; all from Cell Signaling, Beverly, MA) or phosphoGSK3β(Tyr216; Millipore, Billerica, MA). The blots were stripped and reprobed with antibodies to AKT, p44/42 ERK1/2, MEK1/2, or GSK3β (Cell Signaling, Beverly, MA), respectively. The bands were visualized and quantified (Odyssey Infrared Imaging System and Software, Licor Biosciences, Lincoln, NE).

Western blot analysis of γH2AX, PCNA, and actin. Total-protein extract (50 µg) from hepatoma and MCF7(SR$^-$) tumors were size-fractionated (NuPAGE Novex 4% to 12% Bis–Tris Midi Gels, Invitrogen) and transferred onto membranes (IBlot system, Invitrogen). Antibodies to phosphohistone (γH2AX, Ser 139; catalog no. 2577, Cell Signaling), proliferating cell nuclear antigen (PCNA; catalog no. sc25280, Santa Cruz Biotechnology, Santa Cruz, CA), and actin (Sigma Scientific) were used for detection. Bands were visualized and quantified (model MP 4000, Molecular Imager VersaDoc System and Quantity One Software, BioRad Laboratories).

Statistical analysis. All data are presented as mean ± 1 SD and were compared using one-way ANOVA followed by the Student

Neuman–Keul posthoc test using GraphPad Prism software (La Jolla, CA). Differences among group means were considered statistically different when the P value was less than 0.05.

Results

Animal room illumination. Figure 1 A shows typical light entry from the constantly lighted corridor through a translucent observation window into a traditional-design animal room during the dark-phase. In this case, light entry from a lighted corridor through a standard translucent window 10 in. × 12 in. in size on an animal room door facing out to a corridor subjected to 380.7 ± 1.6 lx (156.1 ± 0.7 μW/cm^2; n = 75 measurements) measured as much as 99.8 ± 7.2 lx (40.9 ± 3.0 μW/cm^2) 8 ft within the room during dark-phase, depending on the location of the detector. At 1 m above the floor, eye-level and inside the rodent cage, lighting measured 21.3 ± 0.3 lx (8.75 ± 0.1 μW /cm^2). Mean daytime illuminance values for the rats during the course of this study measured 300.2 ± 6.8 lx (123.1 ± 2.8 μW/cm^2). Figure 1 B is a photo showing the initial animal room LAN contamination at the base and side of doors on our arrival; the mean dark-phase LAN illuminance value, measured during the course of the first 7 tumor passages (F1 through F7), was 59.8 ± 6.1 lx (24.5 ± 2.5 μW/cm^2).

Figure 1 C is a photo image of animal room LAN entry (door-hinge side only) after the initial improvements and modifications to the doors, including the installation of weather stripping seals and removal of lighted equipment (Figure 1 D), followed by installation of door shoes, seeps, and sills; dark-phase LAN was reduced to 6.1 ± 0.2 lx (2.5 ± 0.08 μW/cm^2; F8 tumor generation) and then to 2.4 ± 0.2 lx (1.0 ± 0.08 μW/cm^2, F9 generation) within the animal cage at eye-level and 1 m above the floor with installation of vinyl gaskets and anodized encasements surrounding the interior of the door frame (Figure 1 E). During the final stage, LAN contamination was reduced to nondetectible levels (0 lx) within the room during dark-phase with the installation of the exterior door light-proof curtain (Figure 1 F and G; during F9 generation).

Arterial blood acid–gases and glucose and melatonin levels. Arterial blood pH, pO_2, O_2 saturation, and pCO_2, collected by cardiocentesis at either 0400 or 1600, revealed little or no differences between time points in either strain of rats and therefore are reported here as mean values. Arterial blood pH, pO_2, O_2 saturation, and pCO_2 levels were, respectively, 7.43 ± 0.02, 152.3 ± 3.6 mm Hg, 99.2 ± 0.2%, and 33.2 ± 2.4 mm Hg for male Buffalo rats and 7.45 ± 0.02, 151.8 ± 3.0 mm Hg, 99.2 ± 0.2%, 31.1 ± 2.2 mm Hg for female nude rats. These values were identical to carotid arterial values in blood acid–gases obtained during tumor arterial and venous difference measurements (Table 1). Blood glucose levels, showing a similar trend and slightly elevated at 0400 (nighttime) compared with 1600 (daytime) for both the male Buffalo and female nude rats, were 110.0 ± 1.6 mg/dL (6.11 ± 0.04 mM) and 108.6 ± 1.7 (5.93 ± 0.04 mM), respectively. There was no morbidity as a result of the anesthesia or cardiocentesis during the course of the study, and rats were immediately active after the procedure.

Melatonin concentrations in arterial plasma samples followed similar day–night trends for both strains of rat during the course of this study. Daytime plasma values for male Buffalo and female nude rats were 4.7 ± 0.3 and 8.5 ± 1.5 pg/mL, respectively; these levels were nearly identical to nighttime values (7.5 ± 1.5 and 5.1 ± 0.7 pg/mL, respectively) at the beginning of the study when animal room dark-phase light contamination was highest (exceeding 10 μW/cm^2). Figure 2 depicts changes that occurred in nighttime plasma melatonin levels relative to decreasing LAN due to animal room modifications and improvements. After installation of door seals, shoes, and rubber gaskets (during F8), nighttime melatonin levels in both nude rats and Buffalo rats began to return to normal values, at 82.1 ± 4.5 and 71.9 ± 8.1 pg/mL, respectively, already significantly (P <0.001) higher than levels before elimination of LAN contamination. In the final stages of elimination of LAN contamination, after the addition of the exterior dark curtains, nighttime melatonin levels reached normal values of 123 ± 6.3 and 85.3 ± 1.2 pg/mL for the nude and Buffalo rats, respectively. In both strains of nontumor-bearing rats, nighttime levels rose over 10-fold returning to normal levels (well above 100 pmol/mL), in a direct relationship (r > 0.99) with decreasing LAN values.

Tumor growth rates. Latency-to-onset of tumor growth (when tumors were approximately pea-size) was recorded for each generation, and tumor weights were estimated every other day. During maximal LAN exposure in the animal facility (F1 through F8), latency-to-onset of tumor growth for MCF7(SR$^-$) xenografts and 7288CTC hepatomas were consistently 11 and 5 d, respectively, and tumor growth rates (Figure 3) were 0.60 ± 0.02 and 1.59 ± 0.07 g/d. After installation of door seals, shoes, and gaskets, as dark-phase LAN was reduced to about 6 lx (F8) and then to 2 lx (F9), latency-to-onset of growth and tumor growth rates for MCF7(SR$^-$) xenografts and 7288CTC hepatomas were, respectively, 12 and 9 d and 0.53 ± 0.04 and 1.30 ± 0.03 g/d. After modifications were completed with the installation of the outside light-tight curtain and dark-phase LAN was eliminated completely (F10 to F26), latency-to-onset and tumor growth rates of MCF7(SR$^-$) xenografts and 7288CTC hepatomas were, respectively, 15 and 13 d and 0.26 ± 0.02 and 0.72 ± 0.04 g/d.

Tumor arterial and venous difference measurements. Table 1 depicts arterial glucose supply and tumor glucose uptake; arterial and tumor venous pO_2, pCO_2, and pH in vivo; and measures of rates of metabolism during the light phase of tumor arteriovenous whole-blood collections. Arterial and venous blood flow rates remained constant during the course of collections for both the MCF7(SR$^-$) breast cancer xenografts and 7288CTC hepatomas, measuring 0.130 ± 0.005 and 0.139 ± 0.005 mL/min (arterial), respectively, and 0.125 ± 0.005 and 0.132 ± 0.004 mL/min (venous). Similarly, arterial glucose supply to the tumors remained constant throughout the course of each collection, with arterial blood glucose concentrations in the female nude rats and male Buffalo rats during the light phase at 0600 and 0700 measuring 5.98 ± 0.18 and 6.01 ± 0.13 mM, respectively. In the case of both metabolically active tumors at this time of day, almost 30% and 45% of the available glucose supply to the MCF7(SR$^-$) human breast cancer xenografts and 7288CTC hepatomas, respectively, was taken up. More than 60% of the available supply of oxygen was used during the course of the blood collections, and CO_2 production was nearly 2-fold. Venous pH, acidic compared with arterial pH, was significantly (P < 0.05) different in both tumor types.

Tumor fatty acid metabolism data are presented in Table 2. Tumor cAMP concentrations, elevated during the light phase, revealed no differences after elimination of LAN contamination (after F10) compared with those before (F1 through F8). Arterial plasma concentrations of both total fatty and linoleic acids during the light phase were elevated (P <0.05) before compared with after elimination of LAN contamination. Arterial plasma concentrations of total fatty acids/linoleic acid in nude and Buffalo rats before and after elimination of LAN contamination, respectively, measured 6.35 ± 0.24/1.61 ± 0.06 mM and 5.45 ± 0.14/1.36 ± 0.04 mM (nude rats), and 5.49 ± 0.45/1.97 ± 0.14

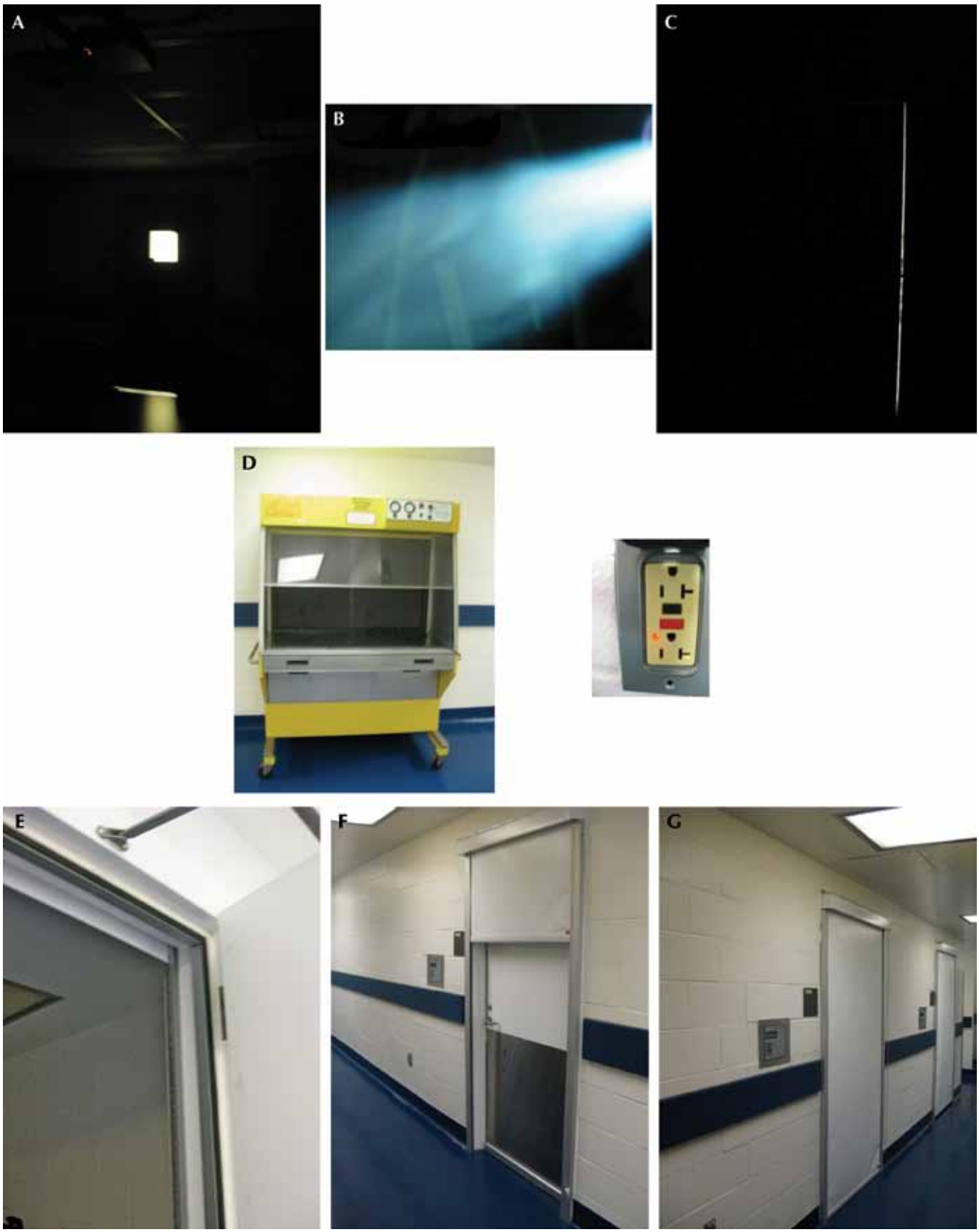

Figure 1. (A and B) Example of a traditional-design animal room door with translucent observation window and light-at-night contamination (LAN) exceeding 50 lx leading into the animal room, LAN contamination exceeding 10 lx around door frame, and modifications and improvements made to the animal rooms, including (D) removal lighted equipment, (E) installation of door frame shoes, seals, and sweeps with vinyl gaskets and anodized aluminum encasements, and (F and G) exterior light-tight curtains.

Table 1. Tumor xenograft hematology data (mean ± 1 SD; n = 6 per group) in vivo during the light phase (0600–1800) after animal room LAN elimination

Tumor xenograft	Arterial glucose supply (μg/min/g)	Glucose uptake		pO_2 (mm Hg)		pCO_2 (mm Hg)		pH	
		μg/min/g	% of arterial supply to tumor	Artery	Vein	Artery	Vein	Artery	Vein
MCF7(SR⁻)	14.8 ± 2.5	4.4 ± 0.9	29.9% ± 3.4%	154.7 ± 7.1	56.4 ± 3.8[a]	30.4 ± 0.9	57.1 ± 4.9[a]	7.45 ± 0.02	7.32 ± 0.01[a]
7288CTC	12.5 ± 1.1	5.6 ± 0.6	44.5% ± 1.1%	153.0 ± 3.3	50.8 ± 4.9[a]	30.0 ± 3.3	60.2 ± 3.9[a]	7.45 ± 0.03	7.31 ± 0.01[a]

MCF7(SR⁻) is a human breast carcinoma xenograft; 7288CTC is a rat hepatoma.
[a]$P < 0.05$ compared with arterial value.

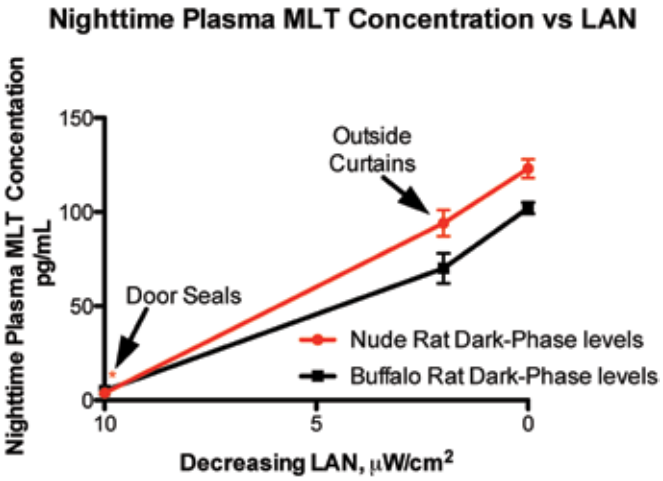

Figure 2. Changes in nighttime plasma melatonin concentration (pg/mL; mean ± 1 SD, n = 6 per group) over time relative to decreasing light-at-night (LAN; μW/cm²) as a result of modifications and improvements made to the animal rooms. Dark-phase plasma melatonin concentrations in adult, female nude rats (red circles) and adult, male Buffalo rats (black squares). Concentrations without asterisks are different ($P < 0.05$) from concentrations with asterisks.

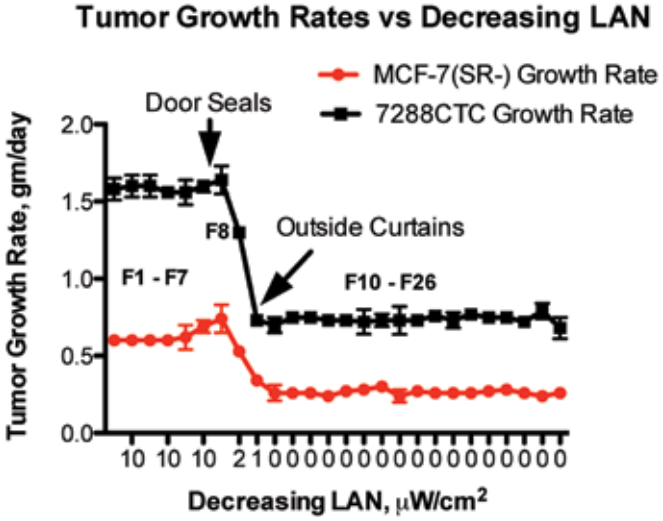

Figure 3. Tumor growth rates (g/d; mean ± 1 SD, n = 6 per group) relative to decreasing light-at-night (μW/cm²) over time as a result of modifications and improvements made to the animal rooms. Tumor growth rates in adult, female nude rats (red circles) and adult, male Buffalo rats (black squares). Growth rates of generations F1 through F9 are different ($P < 0.05$) from those of generations F10 through F26.

and 4.39 ± 0.39/1.60 ± 0.06 mM (Buffalo rats). However, tumor total fatty and linoleic acid uptakes, as percentages of supply to tumors, were more than 10% higher ($P < 0.05$) during the LAN-contamination period (generations F1through F8) as compared with afterward (after F9) in both tumor types. Although linoleic acid uptake as a percentage of total fatty acid uptake remained constant for MCF7(SR⁻) breast tumors and 7288CTC hepatomas before and after elimination of LAN contamination, tumor conversion of linoleic acid to the mitogenic agent 13-HODE and 13-HODE production/linoleic acid utilization were elevated more than 4-fold ($P < 0.05$) in both tumor types in rats exposed to LAN contamination.

Fatty acid contents of MCF7(SR⁻) human breast cancer xenografts and 7288CTC hepatomas. Total fatty acid contents of the MCF7(SR⁻) human breast and 7288CTC rodent hepatoma tumors before elimination of LAN contamination were 3.5- and 6.5-fold higher, respectively, than those after elimination (Table 3). Triglycerides, the principal storage class in both tumors, had significant ($P < 0.001$) decreases in content and composition after, as compared with before, elimination of LAN contamination. In terms of phospholipids and cholesterol ester, fatty acid composition of the lipid component was the same before and after elimination of LAN contamination for individual tumor types. Individual fatty acids, examined as percentages of total triglycerides, were similar before and after elimination of LAN contamination. In all instances, the most abundant fatty acid was linoleic acid, followed by palmitic and oleic acids, and these findings corresponded well with the proportional increase found in blood plasma.

Western blot measurement of tumor phosphorylated kinases. MCF7(SR⁻) human breast cancer xenografts and 7288CTC hepatomas of host animals before and after elimination of LAN contamination showed high daytime expression of phosphorylated forms of ERK 1/2, MEK, and AKT perfused in situ (Figure 4), characteristic of these actively proliferating tissues, and correlated with total fatty and linoleic acid uptakes and 13-HODE release rates (Table 1). Protein analysis of each tumor type revealed no significant differences before and after elimination of LAN contamination; mean values were 5.04 ± 0.36 and 5.84 ± 0.88 μg/μL for MCF7(SR⁻) human breast cancer xenografts and 7288CTC rat hepatomas, respectively.

Western blot analysis of γH2AX, PCNA, and actin. Western blot analysis of γH2AX phosphorylation in MCF7(SR⁻) human breast cancer xenografts and 7288CTC rodent hepatomas derived from rats maintained under LAN or after its elimination demonstrated a statistically significant ($P < 0.05$, t test, 2 samples with equal variance) decrease after LAN elimination (Figure 5) . The same trend ($P = 0.084$) of a decrease in the γH2AX levels was observed in MCF7(SR⁻) samples obtained after elimination of LAN. A similar trend ($P = 0.081$) was detected by Western blot analysis for the proliferation marker PCNA, which is involved in DNA repair.[13,27]

Table 2. Tumor metabolism data (mean ± 1 SD; n = 6 per group) in vivo during daytime (0600–1800) before and after animal room LAN elimination

		cAMP	Total fatty acid uptake		Linoleic acid uptake		13-HODE (ng/min/g)		Linoleic acid/ total fatty acid (%)	13-HODE production/ linoleic acid utilization (%)
		nmol/g tissue	μg/min/g	%	μg/min/g	%	Arterial supply	Venous output		
MCF7(SR⁻)	F1-F7; before LAN elimination	0.94 ± 0.03	4.86 ± 1.19	30.1 ± 1.7	1.07 ± 0.22	30.4 ± 2.8	ND	5.71 ± 0.49	23.0 ± 1.6	0.60 ± 0.11
	F10-F26; after LAN elimination	0.91 ± 0.03	4.78 ± 0.90	21.3 ± 2.1[a]	1.14 ± 0.14	21.9 ± 2.4[a]	ND	1.46 ± 0.43[a]	23.3 ± 0.7	0.13 ± 0.04[a]
7288CTC	F1-F7; before LAN elimination	0.91 ± 0.02	7.01 ± 1.10	52.2 ± 2.9	2.61 ± 0.22	59.9 ± 5.1	ND	5.78 ± 1.35	33.6 ± 1.2	5.19 ± 0.59
	F10-F26; after LAN elimination	0.95 ± 0.04	6.75 ± 1.57	44.1 ± 2.8[a]	2.39 ± 0.33	46.0 ± 1.0[a]	ND	ND[a]	34.8 ± 1.0	1.43 ± 0.17[a]

ND, not detectable
Tumor weight (mean ± 1SD; n = 3): MCF7(SR⁻), 6.7 ± 1.6 g; 7288CTC, 7.6 ± 1.1 g
[a]$P < 0.05$ compared with value before LAN elimination

Table 3. Fatty acid and lipid content (μg/g ; mean ± 1 SD; n = 3) of MCF7(SR⁻) human breast tumors and 7288CTC hepatoma harvested during the light phase before and after elimination of light at night (LAN) contamination

	Fatty acid	Triglycerides		Phospholipids		Free fatty acids		Cholesterol ester		Total fatty acids	
		Before	After	Before	After	Before	After	Before	After	Before	After
MCF7(SR⁻)											
	C14:0	248 ± 20	0	7 ± 1	14 ± 9	3 ± 1	0	3 ± 1	0	260 ± 23[a]	14 ± 8
	C16:0	3523 ± 414	799 ± 331	412 ± 109	457 ± 139	38 ± 1	14 ± 1	8 ± 1	9 ± 2	3981 ± 520[a]	1280 ± 420
	C16:1	599 ± 55	0	73 ± 27	67 ± 17	7 ± 1	0	13 ± 1	10 ± 1	668 ± 88[a]	71 ± 18
	C18:0	1063 ± 135	633 ± 314	294 ± 57	295 ± 51	26 ± 3	16 ± 1.2	11 ± 3	10 ± 1	1424 ± 153[a]	950 ± 358
	C18:1	3240 ± 152	570 ± 35	295 ± 101	806 ± 146	58 ± 10	11 ± 1	9 ± 7	11 ± 4	3602 ± 57[a]	696 ± 245
	C18:2	7044 ± 936	1626 ± 245	469 ± 112	483 ± 118	26 ± 6	22 ± 7	7 ± 3	6 ± 1	7546 ± 1033[a]	2145 ± 334
	C20:4	350 ± 53	0	445 ± 149	365 ± 196	14 ± 3	9 ± 1	20 ± 5	15 ± 1	825 ± 166[a]	386 ± 200
	Total	16336 ± 1880	3448 ± 497	1896 ± 548	1998 ± 541	139 ± 48	65 ± 19	66 ± 4	41 ± 9	18436 ± 2342[a]	5552 ± 901
7288CTC											
	C14:0	1891 ± 89	124 ± 17	100 ± 47	98 ± 15	7 ± 1	0	4 ± 3	3 ± 1	2003 ± 131[a]	182 ± 63
	C16:0	29642 ± 719	2190 ± 299	1755 ± 832	2014 ± 864	323 ± 50	145 ± 33	129 ± 23	119 ± 18	31518 ± 1289[a]	4504 ± 800
	C16:1	7685 ± 1794	425 ± 66	442 ± 203	513 ± 93	56 ± 22	38 ± 17	36 ± 7	33 ± 8	8232 ± 1845[a]	1086 ± 206
	C18:0	4547 ± 148	394 ± 40	318 ± 141	365 ± 89	188 ± 29	243 ± 61	107 ± 10	95 ± 11	5172 ± 268[a]	1098 ± 164
	C18:1	18248 ± 967	1480 ± 72	1383 ± 604	1683 ± 366	142 ± 35	160 ± 58	87 ± 1	82 ± 4	19857 ± 1541[a]	3405 ± 451
	C18:2	40875 ± 1761	2938 ± 835	2816 ± 1181	3457 ± 801	350 ± 56	400 ± 143	230 ± 29	221 ± 27	44270 ± 2874[a]	7015 ± 1052
	C20:4	360 ± 2	0	203 ± 102	183 ± 79	195 ± 67	168 ± 36	90 ± 2	91 ± 14	975 ± 490[a]	306 ± 96
	Total	103660 ± 3900	7552 ± 1203	6812 ± 2947	8314 ± 2307	1240 ± 161	1154 ± 348	577 ± 78	546 ± 46	112293 ± 6690[a]	17188 ± 2396

[a]$P < 0.05$ compared with the value after elimination of LAN contamination

Discussion

Light and alternating light:dark cycles play an integral role in the mammalian environment for laboratory animals and humans alike and can influence the synchronization of a variety of circadian rhythms, all of which are controlled by the suprachiasmatic nucleus.[14,40,57-59] In an intensity-,[11] duration-,[9] and wavelength-dependent[12] manner, light present during nighttime can markedly disrupt chronobiologic rhythms of sleep–activity, feeding, core body temperature, metabolism, hormone production, and cell proliferation.[5,56] Over time, LAN disruption of circadian regulation of the SCN and the nighttime melatonin signal may result in the predisposition to or development of cardiovascular diseases, diabetes, depression, or cancer.[58,67] Although many studies over the years have addressed the direct effects of daytime light on circadian behavior and physiology in mammalian systems, particularly in laboratory animals, the influence of LAN on these parameters is still little understood. Certainly, recent investigations[7-10,16-18,22,23,58] and the imminent arrival of the 2010 edition of *The Guide*[30] may encourage further investigation in this important area. Nonetheless, understanding of and adherence to correct maintenance of controlled lighting and lighting protocols in laboratory animal

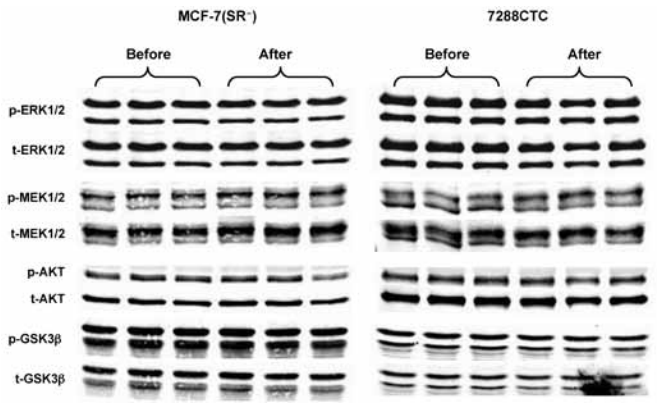

Figure 4. Western blot analyses for the expression of total (t-) and phosphorylated (p-) forms of ERK 1/2 (p44/p42), MEK, AKT, and GSK3β in MCF7(SR^-) human breast cancer xenografts (left panel) or 7288CTC rat hepatomas (right panels) in vivo harvested during the light phase before elimination of LAN contamination (left panels) and after elimination of LAN contamination. Each lane depicts bands from a single tumor.

facilities is of utmost importance to scientific investigators and animal care personnel.

During the relocation and transition to our new cancer research facility, we first had to address the primary issue of LAN contamination in our laboratory animal rooms prior to continuing our investigations. In older animal facilities, doors leading into animal quarters often have considerable light-leaks around door frames, due to unevenness, absence of door seals and gaskets, and uncovered observation windows. These leaks allow light entry from the outside environment, which includes constantly lighted corridors.[22] Indeed, as shown in the current investigation, even minor LAN entry through a standard, uncovered observation window can create enough LAN within the animal cage to markedly influence rodent circadian regulation.[3,5,10,25,58] As simple and inexpensive modifications and improvements to our animal rooms to eliminate LAN contamination were completed, disruptions in circadian regulation in animal and tumor physiology and metabolism resolved. We were able to follow and document these changes by using the well-defined, sensitive animal metabolic and physiologic indicators of host plasma melatonin levels and tumor latency-to-onset of growth and growth rates for both the human and rodent tumors we studied.[7,16,18]

The original studies on this topic reported that rodents (at least white albino rodents) must receive at least 5 to 10 lx (2.05 to 4.1 $\mu W/cm^2$) during light phase and no more than 0.15 to 0.2 lx (0.6 to 0.08 $\mu W/cm^2$) during dark phase to sustain photoperiodicity, as measured by sleep–wake cycle and locomotor activity.[40,46] However, the same studies showed that exposure to LAN of 0.2 lx or more for even a few seconds is sufficient to cause an immediate suppression of the melatonin signal; however, alterations in circadian rhythms of metabolism and physiology were not measured. Since that initial work, much more has been done using a variety of mammalian species and more sensitive analyses and has revealed that synchrony and disruption of circadian rhythms in mammals are associated with much lower levels of light during both the daytime and nighttime.[6,10,16,18,26,59] Most recently, a study demonstrated that as little as 0.2 lx (0.08 $\mu W/cm^2$) LAN during dark-phase was sufficient to cause major disruptions in circadian regulation of blood physiology and metabolism in Sprague–Dawley rats[17] and human breast tumor[7,8] and rodent hepatoma 7288CTC[7,8,16,18] metabolism and proliferation in vivo. Even sodium yellow lamps (570 nM)[43] and red safety-lamps (above 650 nM),[28] also in common use for dark-phase observation purposes, can dramatically suppress the normal nighttime melatonin signal, in turn causing disruptions in rodent circadian metabolic homeostasis.

Duration[10] and wavelength[12] of nighttime light exposure play a key role in the regulation of the normal, nighttime physiologic levels of melatonin, which functions as an important and sensitive indicator of normal circadian rhythmicity and in daily reentrainment of the suprachiasmatic nucleus. Exposure of rodents to as little as 1 h of incandescent light at night or alternating dim red light[3] alters corticosterone, glucose, and lactic acid levels.[17] Some investigators have shown that, by altering daily rhythms of dietary intake or subjecting animals to hypothalamic lesions, SCN-generated rhythms blood glucose and insulin are independent of both feeding and activity cycles.[1,21,37,39,66] Rats exposed to even low levels of dark-phase LAN contamination, much like pinealectomized animals which lack a melatonin signal, no longer exhibit normal daily rhythms of fatty acid, glucose, lactic acid,[17,21,38] insulin,[4,21,38,40,50] and corticosterone levels,[17,63] with glucose concentrations remaining elevated throughout the 24-h day.[17] Recent evidence reveals that some strains of mice appear to exhibit similar LAN-induced disruptions.[23] Although we did not measure 24-h rhythms of arterial blood glucose concentrations, tumors with elevated glucose uptake rates hypothetically also would have increased rates of metabolism, compared with tumors sampled after elimination of LAN contamination; we demonstrated these effects on metabolism here through the elevated rates of O_2 uptake and CO_2 production. Removing the nighttime source of melatonin in rodents causes a decrease in hepatic and muscular glycogenesis[70] and increases plasma concentrations of glucose and glucagon.[21] In a previous investigation,[17] we showed that animals subjected to LAN of as little as 0.2 lx (0.08 $\mu W/cm^2$) had plasma glucose levels that were phase-altered, with the time of peak concentration at 1600 and the nadir at 0400. The human breast cancer xenografts and rat hepatomas both showed concomitantly high rates of oxygen consumption and CO_2 production during the light phase, indicating normal rates of respiration for these tumors.[7,8,16,18,61,62]

Greater daily availability of plasma fatty acids, as measured before compared with after elimination of LAN contamination, led to greater than 300- and 600-fold increases in tumor total fatty acids and lipid content of human breast cancer xenografts and rat hepatomas, respectively. Such disruptions in normal tumor diurnal fatty acid synthesis and storage capacity, as observed in earlier studies of animal exposed to controlled LAN environments,[7,16,18] suggest an altered metabolic state, predisposing the tumors to more rapid proliferation. Before elimination of LAN contamination, human breast cancer xenografts and rat hepatomas showed high rates of both total fatty and linoleic acid uptakes of nearly 10% (utilization compared with supply), and 13-HODE production was nearly 4-fold and 22-fold higher, respectively, compared with uptakes after elimination of LAN contamination. In addition, 13-HODE production/linoleic acid utilization rates were more than 3-fold higher in both tumors before compared with after elimination of LAN contamination, similar to previous findings reported for these tumors in animals in either a light:dark (12:12-0.2 lx) or constant bright light (24:0) environment.[7,8,16,18,62] These higher rates of tumor 13-HODE production and 13-HODE production/linoleic acid utilization, in conjunction with the increased rates of linoleic acid uptake by the tumors of animals before compared with after elimination of LAN conditions, argue for a metabolic shift in linoleic acid utilization by the tumors in the LAN-exposed animals. Fatty

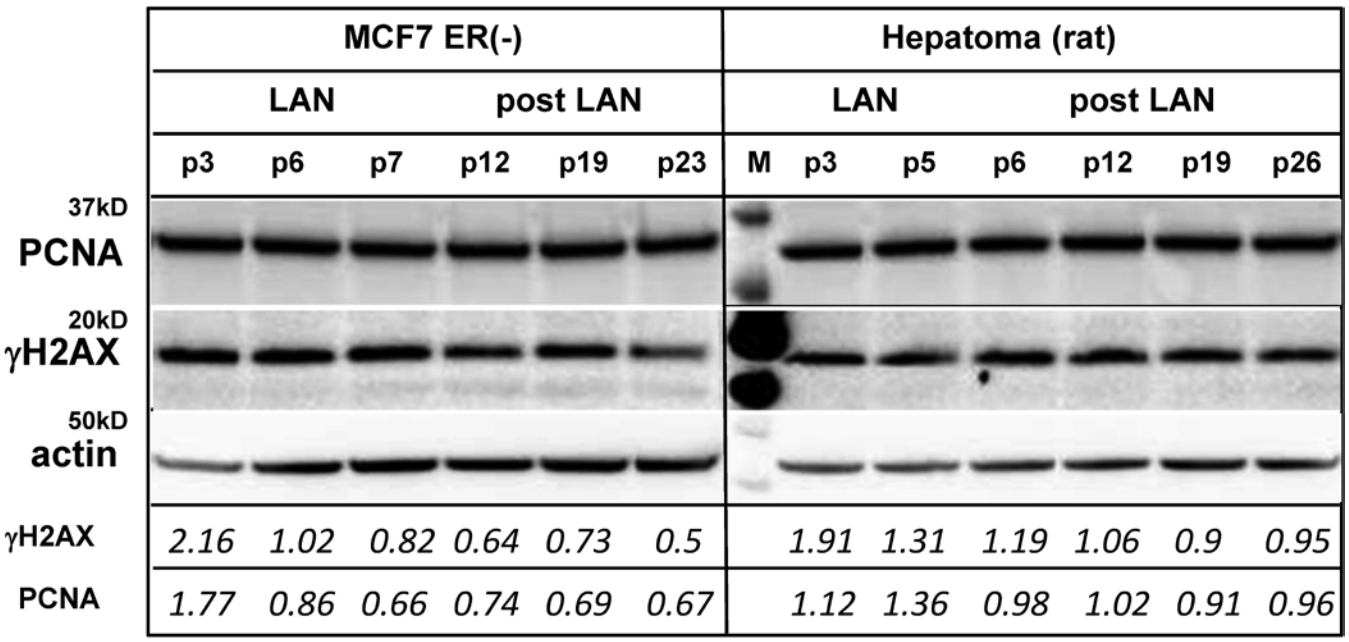

Figure 5. Assessment of proliferation and DNA damage markers in rat hepatomas and human breast cancer xenograft tumors harvested during the light phase from rats maintained before or after elimination of LAN. Protein samples extracted from tumors [rat hepatoma or MCF7(SR$^-$) breast cancer xenografts] of different passages were analyzed by Western blot for PCNA and actin expression and for γH2AX phosphorylation. Protein samples derived from tumors from passages 3, 5, and 6 (hepatoma) and 3, 6, 7 [MCF7(SR$^-$)] originated from rats maintained before elimination of LAN. Protein samples derived from tumors from passages 12, 19, and 26 (hepatoma) and 12, 19, and 23 [MCF7(SR$^-$)] originated from rats maintained after elimination of LAN. Each lane depicts phosphorylated PCNA, γH2AX, or actin from a single tumor. Numbers at the bottom represent relative levels of γH2AX or PCNA for each passage (normalized to actin). Numbers on the left side of the figure correspond to the size of the protein marker (M). γH2AX levels differed significantly ($P < 0.05$, t test of 2 samples with equal variance) between hepatoma samples obtained before and after elimination of LAN.

acids stored by the MCF7 (SR$^-$) human breast cancer xenografts and 7288CTC rat hepatomas serve as a remarkable source of fuel, whereas the glycerol released is used in gluconeogenesis by the liver.[71]

Increased uptake of linoleic acid, as determined here in tumors of rats maintained in the room before elimination of LAN contamination, is linked directly to the activation of MEK, ERK 1/2, and AKT. Activation of these molecules in the insulin growth factor and epidermal growth factor receptor signaling pathways, along with the clock gene-associated GSK3β kinase, was not examined during the dark-phase either before or after elimination of LAN. However, a previous investigation[7] has shown that the signaling molecules MEK and ERK 1/2 are activated continuously in tumors of animals exposed to LAN or a constant bright-light environment. Presumably, this would also be the case with GSK3β, suggesting concomitant upregulation of numerous metabolic pathways associated with cell proliferation.

Tumor growth is associated with cell division that leads to generation of double-stranded DNA breaks due to stalled replication forks and other intrinsic DNA-damaging factors. γH2AX phosphorylation is one of the first steps in the signaling response to double-stranded DNA breaks,[60] and it is often used as a marker of this type of DNA damage.[55] The hepatoma 7288CTC is a highly undifferentiated rat tumor,[7,62] with elevated growth rates under normal conditions (approximately 0.7 g/d),[16,18] as compared with that of the MCF7(SR$^-$) human breast cancer (0.25 g/d),[6-8,17,62] a poorly differentiated, grade 3, ductal breast adenocarcinoma.[8] Indeed, γH2AX and PCNA phosphorylation activity may well be associated to some degree with the normal proliferative activity of both tumor types during the light phase. To our knowledge, the current study is the first examination of γH2AX phosphorylation in these tumor tissues in animals exposed to a constant LAN environment. These data are consistent with previous reports of increased tumor growth in animals exposed to LAN.[7,16,18]

Relocating a laboratory animal science research program to a new institution can be a daunting task when dealing with controlled lighting environments and eliminating LAN contamination. The consistency and quality of lighting intensity, wavelength, and duration during controlled photoperiods, are of utmost importance in maintaining normal, healthy animal biologic rhythms of metabolism and physiology and in influencing the outcome of scientific investigations. During the course of our relocation, LAN contamination factors, such as translucent observation windows; lighted in-room electrical equipment; and leaky door jams, sills and frames, had to be eliminated before we could move forward with our in vivo cancer research investigations. Our study provides compelling evidence that these issues can be systematically and successfully resolved through close collaborative efforts and cooperation between scientific investigators and vivarium technical and administrative personnel. The findings presented here advance our understanding of the influence of environmental LAN on circadian regulation of metabolism and physiology and will encourage improved facility design and lighting protocols, to ensure the credible outcome of scientific investigations.

Acknowledgments

We express our sincere gratitude and heartfelt thanks for the exceptional assistance during the course of the laboratory transition period, especially to Rosezina L Almanza, Sheena Gauthreaux, Michael J Webb, and all the superb staff of the Tulane University School of Medicine Department of Comparative Medicine, and to Deborah Lauff and Shannon Dawsey of the Department of Structural and Cellular Biology. Without their able assistance, our successful relocation and human cancer re-

search investigations would not have been possible.

This work was supported in part by a Tulane University School of Medicine and Louisiana Cancer Research Consortium Startup Grant (no. 631455 to DEB), NIH grant (no. P20RR020152), National Institute on Aging grant (no. 5K01AG030074-02 to VPB), the Ellison Medical Foundation New Scholar in Aging Award (no. 547305G1 to VPB), and the American Association for Laboratory Animal Science Grants for Laboratory Animal Science (GLAS) Award (to RTD).

References

1. **Acuna-Castroviejo D, Reiter RJ, Menedez-Pelaez A, Pablos MI, Burgos A.** 1994. Characterization of high-affinity melatonin binding sites in the purified cell nuclei of rat liver. J Pineal Res **16:**100–112.
2. **Aschoff J.** 1960. Exogenous and endogenous components in circadian rhythms. Cold Spring Harb Symp Quant Biol **25:**11–28.
3. **Aschoff J, editor.** 1981. Handbook of behavioral neurobiology, biological rhythms, p 1–581. New York (NY): Plenum Press.
4. **Bailey CJ, Atkins TW, Matty AJ.** 1974. Melatonin inhibition of insulin secretion in the rat and mouse. Horm Res **5:**21–28.
5. **Bellhorn RW.** 1980. Lighting in the animal environment. Lab Anim Sci **30:**440–450.
6. **Berson DM, Dunn FA, Takao M.** 2002. Phototransduction by retinal ganglion cells that set the circadian clock. Science **295:**1070–1073.
7. **Blask DE, Brainard GC, Dauchy RT, Hanifin JP, Davidson LK, Krause JA, Sauer LA, Rivera-Bermudez MA, Dubocovich ML, Jasser SA, Lynch DT, Rollag MD, Zalatan F.** 2005. Melatonin-depleted blood from premenopausal women exposed to light at night stimulates growth of human breast cancer xenografts in nude rats. Cancer Res **65:**11174–11184.
8. **Blask DE, Dauchy RT, Sauer LA, Holowachuk E, Ruhoff M, Kopff H.** 1999. Melatonin inhibition of cancer growth in vivo involves suppression of tumor fatty acid metabolisms receptor-mediated signal transduction events. Cancer Res **59:**4693–4701.
9. **Brainard GC. 1989.** Illumination of laboratory animal quarters: participation of light irradiance and wavelength in the regulation of the neuroendocrine system, p 69–74. In: Guttman HN, Mench JA, Simmonds RC, editors. Science and animals: addressing contemporary issues. Bethesda (MD): Scientists Center for Animal Welfare.
10. **Brainard GC, Hanifin JP, Greeson JM, Byrne B, Glicman G, Gerner E, Rollag MD.** 2001. Action spectrum for melatonin regulation in humans: evidence for melatonin a novel circadian photoreceptor. J Neurosci **21:**6405–6412.
11. **Brainard GC, Richardson BA, King TS, Matthews SA, Reiter RJ.** 1983. The suppression of pineal melatonin content and N-acetyl-transferase activity by different light irradiances in the Syrian hamster: a dose-response relationship. Endocrinology **113:**293–296.
12. **Brainard GC, Richardson BA, King TS, Reiter RJ.** 1984. The influence of different light spectra on the suppression of pineal melatonin content in the Syrian hamster. Brain Res **294:**333–339.
13. **Bravo R, Frank R, Blundell PA, Macdonald-Bravo H.** 1987. Cyclin/PCNA is the auxiliary protein of DNA polymerase δ. Nature **326:**515–517.
14. **Carrillo-Vico A, Guerrero JM, Lardone PJ, Reiter RJ.** 2005. A review of the multiple actions of melatonin on the immune system. Endocrine **27:**189–200.
15. **Clough G.** 1982. Environmental effects on animals used in biomedical research. Biol Rev Camb Philos Soc **57:**487–523.
16. **Dauchy RT, Blask DE, Sauer LA, Brainard GC, Krause JA.** 1999. Dim light during darkness stimulated tumor progression by enhancing tumor fatty acid uptake and metabolism. Cancer Lett **144:**131–136.
17. **Dauchy RT, Dauchy EM, Tirrell RP, Hill CR, Davidson LK, Greene MW, Tirrell PC, Wu J, Sauer LA, Blask DE.** 2010. Dark-phase light contamination disrupts circadian rhythms in plasma measures of physiology and metabolism. Comp Med **60:**348–356.
18. **Dauchy RT, Sauer LA, Blask DE, Vaughan GM.** 1997. Light contamination during the dark phase in 'photoperiodically controlled' animal rooms: effect on tumor growth and metabolism in rats. Lab Anim Sci **47:**511–518.
19. **De Boer SF, Van der Gugten J.** 1987. Daily variations in plasma noradrenaline, adrenaline, and corticosterone concentrations in rats. Physiol Behav **40:**323–328.
20. **Depres-Brummer P, Levi F, Metger G, Touitou Y.** 1995. Light-induced suppression of the rat circadian system. Am J Physiol **268:**R1111–R1116.
21. **Diaz B, Blazquez E.** 1986. Effect of pinealectomy on plasma glucose, insulin, and glucagon levels in the rat. Horm Metab Res **18:**225–229.
22. **Faith RE, Huerkamp MJ.** 2008. Environmental considerations for research animals, p 59–83. In: Hessler JR, Lehner NDM, editors. Planning and designing research animal facilities. Burlington (MA): Academic Press.
23. **Fonken LK, Workman JL, Walton JC, Weil ZM, Morris JS, Haim A, Nelson RJ.** 2010. Light at night increases body mass by shifting the time of food intake. Proc Natl Acad Sci USA **107:**18664–18669.
24. **Frye RA.** 1999. Characterization of 5 human cDNAs with homology to the yeast *SIR2* gene: Sir2-like proteins (sirtuins) metabolize NAD and may have protein ADP–ribosyltransferase activity. Biochem Biophys Res Commun **260:**273–279.
25. **Hastings MH, Reddy AB, Maywood ES.** 2003. A clockwork web: circadian time in brain and periphery, in health and disease. Nat Rev Neurosci **4:**649–661.
26. **Hattar S, Liao H-W, Takao M, Berson DM, Yau K-W.** 2002. Melanopsin-containing retinal ganglion cells: architecture, projections, and intrinsic photosensitivity. Science **295:**1065–1070.
27. **Hoege C, Pfander B, Moldovan GL, Pyrowolakis G, Jentsch S.** 2002. RAD6-dependent DNA repair is linked to modification of PCNA by ubiquitin and SUMO. Nature **419:**135–141.
28. **Hofstetter JR, Hofstetter AR, Hughes AM, Mayeda AR.** 2005. Intermittent long-wavelength red light increases the period of daily locomotor activity in mice. J Circadian Rhythms **3:**8–16.
29. **Illnerova H, Vanecek J, Hoffman K.** 1983. Regulation of the pineal melatonin concentration in the rat (*Rattus norvegicus*) and the Djungarian hamster (*Phodopus sungorus*). Comp Biochem Physiol A Comp Physiol **74:**155–159.
30. **Institute for Laboratory Animal Research.** 1996. Guide for the care and use of laboratory animals. Washington (DC): National Academies Press.
31. **Ivanisevic-Milovanovic OK, Demajo M, Karakasevic A, Pantic V.** 1995.The effect of constant light on the concentration of catecholamines of the hypothalamus and adrenal glands, circulatory hardenocorticotropin homone, and progesterone. J Endocrinol Invest **18:**378–383.
32. **Jin X, Shearman LP, Weaver DR, Zylka MJ, deVries GJ, Reppert SM.** 1999. A molecular mechanism regulating rhythmic output from the suprachiasmatic circadian clock. Cell **96:**57–68.
33. **Jung B, Ahmad N.** 2006. Melatonin in cancer management: progress and promise. Cancer Res **66:**9789–9793.
34. **Kalsbeek A, Strubbe JH.** 1998. Circadian control of insulin secretion is independent of the temporal distribution of feeding. Physiol Behav **63:**553–558.
35. **Kennaway DJ, Voultsios A, Varcoe TJ, Moyer RW.** 2002. Melatonin in mice: rhythms, response to light, adrenergic stimulation, and metabolism. Am J Physiol Regul Integr Comp Physiol **282:**R358–R365.
36. **Knutsson A, Akerstedt T, Jonsson BG, Orth-Gomer K.** 1986. Increased risk of ischaemic heart disease in shift workers. Lancet **2:**89–92.
37. **La Fleur SE, Kalsbeek A, Wortel J, van der Vliet J, Bujis RM.** 2001. Role for the pineal and melatonin in glucose homeostatsis: pinealectomy increases nighttime glucose concentrations. J Neuroendocrinol **13:**1025–1032.
38. **Li JC, Xu F.** 1997. Influence of light–dark shifting on the immune system, tumor growth, and lifespan of rats, mice, and fruit flies as well as on the counteraction of melatonin. Biol Signals **6:**77–89.
39. **Lima FB, Machado UF, Bartol I, Seraphim PM, Sumida DH, Moraes SM, Hell NS, Okamoto MM, Saad MJ, Carvalho CR, Cipolla-Neto J.** 1998. Pinealectomy causes glucose intolerance

and decreases adipose cell responsiveness to insulin in rats. Am J Physiol **275:**E934–E941.

40. **Lynch HJ.** 1998. The mammalian circadian system and the role of environmental illumination, p 69–87. In: Holley DC, Winget CM, Leon HA, editors. Lighting requirements in microgravity—rodents and nonhuman primates. Washington (DC): National Aeronautics and Space Administration.
41. **Maestroni GJ.** 1995. T-helper-2 lymphocytes: a peripheral target of melatonin. J Pineal Res **18:**84–89.
42. **McEachron DL, Tumas KM, Blank KJ, Prytowsky MB.** 1995. Environmental lighting alters the infection process in an animal model of AIDS. Pharmacol Biochem Behav **51:**947–952.
43. **McLennan IS, Taylor-Jeffs J.** 2004. The use of sodium lamps to brightly illuminate mouse houses during their dark phases. Lab Anim **38:**384–392.
44. **Menaker M.** 1976. Physiological and biochemical aspects of circadian rhythms. Fed Proc **35:**2325–2357.
45. **Milcu SM, Nana-Ionescu I, Milcu I.** 1971. The effect of pinealectomy on the plasma insulin in rats, p 345–357. In: Woltensholme GEW, Knight J, editor. The pineal gland. Edinburgh (UK): Churchill Livingston.
46. **Minneman KP, Lynch HJ, Wurtman RJ.** 1974. Relationship between environmental light intensity and retina-mediated suppression of rat pineal serotonin-N-acetyltransferase. Life Sci **15:**1791–1796.
47. **Mori W, Aoyama H, Murase T, Mori W.** 1989. Antihypercholesterolemic effect of melatonin in rats. Acta Pathol Jpn **39:**613–618.
48. **National Research Council.** 1995. Nutrient requirements of laboratory animals, p 11–79. Washington (DC): National Academies Press.
49. **O'Steen WK, Anderson KV.** 1972. Photoreceptor degeneration after exposure of rats to incandescent illumination. Z Zellforsch Mikrosk Anat **127:**306–313.
50. **Peschke E, Fautek JD, Musshoff U, Schmidt F, Beckmann A, Peschke D.** 2000. Evidence for a melatonin receptor within pancreatic islets of neonate rats: functional, autoradiographic, and molecular investigations. J Pineal Res **28:**156–164.
51. **Piacsek BE, Hautzinger GM.** 1974. Effects of duration, intensity and spectrum of light exposure on sexual maturation time of female rats. Biol Reprod **10:**380–387.
52. **Pittendrigh CS.** 1965. On the mechanism of the entrainment of a circadian rhythm by light cycles, p 277–297. In: Aschoff J, editor. Circadian clocks. Amsterdam (the Netherlands): Elsevier.
53. **Radzialowski FM, Bousquet WF.** 1968. Daily rhythmic variation in hepatic drug metabolism in the rat and mouse. J Pharmacol Exp Ther **163:**229–238.
54. **Redon CE, Dickey JS, Bonner WM, Sedelnikova OA.** 2009. γH2AX as a biomarker of DNA damage induced by ionizing radiation in human peripheral blood lymphocytes and artificial skin. Adv Space Res **43:**1171–1178.
55. **Reiter RJ.** 1973. Comparative effects of continual lighting and pinealectomy on the eyes, the Harderian glands, and reproduction in pigmented and albino rats. Comp Biochem Physiol A Comp Physiol **44:**503–509.
56. **Reiter RJ.** 1991. Pineal melatonin: cell biology of its synthesis and of its physiological interactions. Endocr Rev **12:**109–131.
57. **Reiter RJ.** 1991. Pineal gland: interface between photoperiodic environment and the endocrine system. Trends Endocrinol Metab **2:**13–19.
58. **Reiter RJ.** 2002. Potential biological consequences of excessive light exposure: melatonin suppression, DNA damage, cancer, and neurodegenerative diseases. Neuroendocrinol Lett **23:**9–13.
59. **Reppert SM, Weaver DR.** 2002. Coordination of circadian timing in mammals. Nature **418:**935–941.
60. **Rogakou EP, Pilch DR, Orr AH, Ivanova VS, Bonner WM.** 1998. DNA double-stranded breaks induce histone H2AX phosphorylation on serine 139. J Biol Chem **273:**5858–5868.
61. **Sauer LA, Dauchy RT.** 1988. Identification of linoleic and arachidonic acids as the factors in hyperlipemic blood that increases the [^{3}H]thymidine incorporation in hepatoma 7288CTC perfused in situ. Cancer Res **48:**3106–3111.
62. **Sauer LA, Dauchy RT, Blask DE, Armstrong BJ, Scalici S.** 1999. 13-Hydroxyoctadienoic acid is the mitogenic signal for linoleic acid-dependent growth in rat hepatoma 7288ctc in vivo. Cancer Res **59:**4688–4692.
63. **Seggie J, Sha BE, Uhler I, Brown GM.** 1974. Baseline 24-hour plasma corticosterone rhythm in normal, sham-operated, and septally lesioned rats. Neuroendocrinology **15:**51–61.
64. **Semple-Rowland SL, Dawson WW.** 1987. Retinal cyclic light damage threshold for albino rats. Lab Anim Sci **37:**289–298.
65. **Shapiro C, Girdwood P.** 1981. Protein synthesis in rat brain during sleep. Neuropharmacology **20:**457–460.
66. **Stephan FK, Zucker I.** 1972. Circadian rhythms in drinking behavior and locomotor activity of rats are eliminated by hypothalamic lesions. Proc Natl Acad Sci USA **69:**1583–1586.
67. **Takahashi JS, Hong HK, Ko CH, McDearmon EL.** 2008. The genetics of mammalian circadian order and disorder: implications in physiology and disease. Nat Rev Genet **9:**764–775.
68. **Takeo Y.** 1984. Influence of continuous illumination on estrus cycle in rats: time course of changes in levels of gonadotropins and ovarian steroids until occurrence of persistent estrus. Neuroendocrinology **39:**97–104.
69. **Toklu H, Deniz M, Yuksel M, Keyer-Uysal M, Sener G.** 2009. The protective effect of melatonin and amlodipine against cerebral ischemia–reperfusion-induced oxidative brain injury in rats. Marmara Med J **22:**34–44.
70. **Van Cauter E.** 1998. Putative roles of melatonin in glucose regulation. Therapie **53:**467–472.
71. **Vander Heiden MG, Cantley LC, Thompson CB.** 2009. Understanding the Warburg effect: the metabolic requirements of cell proliferation. Science **324**:1029–1033.